

ZrO₂/hydroxyapatite coating on titanium by electrolytic deposition

Hsueh-Chuan Hsu · Shih-Ching Wu ·
Chih-Hsiung Yang · Wen-Fu Ho

Received: 3 June 2008 / Accepted: 23 September 2008 / Published online: 14 October 2008
© Springer Science+Business Media, LLC 2008

Abstract In this study, hydroxyapatite (HA) was coated on a titanium (Ti) substrate over a ZrO₂ layer by the electrolytic deposition method, this double layer coating was then compared with a single layer coating of HA. The HA layer was used to increase the bioactivity and osteoconductivity of the Ti substrate, and the ZrO₂ layer was intended to improve the bonding strength between the HA layer and Ti substrate, and to prevent the corrosion of the Ti substrate. The electrolytic deposition formed an HA layer with a thicknesses of approximately 20 μm, which adhered tightly to the Ti substrate. The bonding strength of the HA/ZrO₂ double layer coating on Ti was markedly improved when compared to that of the HA single coating on Ti. The improvement in bonding strength with the use of a ZrO₂ base layer was attributed to the resulting increase in chemical affinity of the ZrO₂ to the HA layer and to the Ti substrate. The osteoblast-like cells cultured on the HA/ZrO₂ coating surface, proliferated in a similar manner to those on the HA single coating and on the pure Ti surfaces. At the same time, the corrosion resistance of Ti was improved by the presence of the ZrO₂ coating, as shown by a potentiodynamic polarization test.

1 Introduction

Because of their good mechanical properties, excellent corrosion resistance and biocompatibility, titanium (Ti) and its alloys are widely used for medical and dental applications [1, 2]. However, they are not easily integrated with bone tissue, and much effort has gone into the modification of the Ti surface to improve the implant-tissue osteointegration [3–5]. As a result, bioactive ceramic coatings have been widely used on metal alloys in order to enhance their bioactive potential [6]. Among the various methods which have been used to improve the osteointegration, hydroxyapatite (HA, Ca₁₀(PO₄)₆(OH)₂) coatings have shown good fixation to the bone [7]. This improved biocompatibility is due to the chemical and biological similarity of HA to hard tissues, and its consequent direct bonding to bone [8].

HA is widely used as a bioceramic in orthopedic and dental surgery due to its good biocompatibility and osteoconductivity. It also has the advantage of having a similar chemical composition to the inorganic component of natural bones and teeth [7]. Therefore, a number of researchers have tried to develop new biomaterials which combine the osteoconductive properties of bioactive ceramics with the favorable mechanical properties of Ti and its alloys for clinical applications. The high strength of the Ti and its alloys, and the osteoconductive properties of bioactive ceramics make HA coated Ti implants highly suitable for orthopedic and dental work.

Plasma spray has been conventionally employed for HA coating on Ti implant surfaces. However, this method has some problems for long-term application in implants, such as poor HA crystallinity and weak coating-substrate bond strength. Poor HA crystallinity results from the formation of partially amorphous calcium phosphate crystalline phases which are distinct from that of HA, caused by the

H.-C. Hsu · S.-C. Wu
Department of Dental Laboratory Technology, Central Taiwan
University of Science and Technology, Taichung, Taiwan, ROC

H.-C. Hsu · S.-C. Wu · C.-H. Yang
Institute of Biomedical Engineering and Material Science,
Central Taiwan University of Science and Technology,
Taichung, Taiwan, ROC

W.-F. Ho (✉)
Department of Materials Science and Engineering,
Da-Yeh University, No. 112, Shanjiiao Rd., Dacun,
Changhua 51591, Taiwan, ROC
e-mail: fujii@mail.dyu.edu.tw

extremely high temperatures required for the procedure. Weak coating-substrate bond strength results from the poor adhesion of the plasma-sprayed HA coating to Ti substrate due to the delamination of HA coating from the metal implant [9, 10].

Thus, new HA coating methods have been developed in recent years to replace high temperature plasma spraying techniques [11]. These include, sol-gel processes [12, 13], and electrochemical methods [14–16]. Although, the sol-gel method of forming coatings does have its advantages, electrolytic deposition was employed for the development of ZrO₂/HA coatings in this study because it has specific advantages, such as flexibility of coating highly irregular objects, arbitrary control of coating thickness and chemical composition. After deposition, the coatings were subjected to analysis to determine their electrochemical, structural and mechanical behavior. Furthermore, in order to assess the cell viability, the cellular responses to the coatings were evaluated.

2 Experimental

2.1 Preparation of substrate and deposition

Metal discs (16 mm diameter, 1 mm thickness) of commercially pure titanium (grade 2) were mechanically polished to a mirror finish to facilitate later electrolytic deposits. Before deposition, all substrates were ultrasonically cleaned in double-distilled water and acetone for 10 min, respectively.

The electrochemical deposition was carried out with a potentiostat (AUTOLAB PGSTAT 30, Eco Chemie BV, Netherlands). The titanium discs were used as the working electrode, a platinum wire as the counter electrode, and a saturated calomel electrode (SCE) as the reference electrode. First, the 0.0625 M ZrO(NO₃)₂ · 2H₂O electrolyte was used to form a ZrO₂ coating. Then, the HA coating was made in a solution composed of 0.042 M Ca(NO₃)₂ · 4H₂O and 0.025 M · NH₄H₂PO₄ in double-distilled water. After deposition, the specimens were dried for 24 h and then annealed at 350°C for 1 h in an argon environment.

2.2 Characterization of the coatings

The Hitachi S-3000N scanning electron microscope (SEM) equipped for energy dispersive spectroscopy (EDS) was used for the microstructural analysis. All the ceramic-coated specimens were subjected to SEM/EDS analysis of chemical composition and surface morphology. X-ray diffraction (XRD) was performed on the ceramic-coated specimens using an X-ray diffractometer with CuK_α

radiation operated at 30 kV (voltage) and 20 mA (current) with a scanning speed of 1°/min. The various phases of the specimens were identified by matching each characteristic XRD peak with those in JCPDS files.

In order to test tensile bond strength, the coatings were tested using a standard adhesion test (ASTM C-633). The facings of the loading fixtures were attached to the surface of the coatings with adhesive glue (METCO EP-15). After curing and hardening of the bonding glue, the assembly was loaded in a universal mechanical tester (Instron, AG-IS, SHIMADZU, Japan) for measurement of the tensile bond strength. Six samples per coating type were used for the determination of tensile bond strength. The tensile test was performed at a crosshead speed of 1 mm/min. Cross-section examination of the coatings was performed by slicing, mounting, and polishing a set of 5 cm × 5 cm substrates, followed by examination with scanning electron microscope.

The electrochemical behavior of the samples in the present experiment was tested using potentiodynamic measurement. The electrochemical cell consisted of a working electrode, a saturated calomel reference electrode (SCE), and a platinum counter electrode. The electrochemical tests of the ZrO₂-coated, ZrO₂/HA-coated and uncoated specimens were conducted in artificial saliva at 37°C. The composition of the artificial saliva was: NaCl (400 mg/l), KCl (400 mg/l), CaCl₂ · 2H₂O (795 mg/l), NaH₂PO₄ · H₂O (690 mg/l), KSCN (300 mg/l) and Na₂S · 9H₂O (5 mg/l), with the addition of lactic acid to achieve a pH of 5.5. The electrochemical polarization curves were determined with a potentiostat and associated computer software for corrosion measurements. A scan rate of 0.01 V/s was used in the range of –1.2 to 2.3 V (SCE).

In order to test for biocompatibility, five specimens were used for this test. MG-63 osteoblast-like cells were cultured in Dulbecco's Modified Eagle Medium (DMEM) containing 10% fetal bovine serum, 1% penicillin/streptomycin, 1% L-glutamine and 1% non-essential amino acids in an incubator containing 95% air and 5% CO₂ at 37°C. The cells were cultured and put in direct contact with the specimens. After they were co-cultured for 6 h, the specimens were fixed in 4% formaldehyde solution for 48 h and dehydrated in increasing ethanol concentrations (30–100%). Finally, the surfaces of the culture specimens were gold-sputtered and examined by SEM.

Data which reflected the corrosion potential (E_{corr}), corrosion current density (I_{corr}) and polarization resistance were collected and analyzed by the potentiostat software. One-way ANOVA statistical analysis was used to evaluate the statistical significance of the bond strength and electrochemical data. All results were considered significant ($P < 0.05$).

3 Results and discussion

3.1 HA and ZrO₂ coating characteristics

Figure 1 shows the SEM morphology of the HA/ZrO₂ double layer coating on the Ti substrate. When ZrO₂ was coated onto the Ti substrate at a heat treatment temperature of 350°C, a very thin ZrO₂ coating layer was found, which appeared to be highly dense and relatively uniform. After coating the HA over the ZrO₂ layer and heat-treating the sample at 350°C, the surface appeared to have a plate-like structure (Fig. 1a). The cross-section view clearly shows the formation of the HA/ZrO₂ double layer on the Ti substrate (Fig. 1b). The thickness of the combined HA and ZrO₂ layers was approximately 20 μm. Each layer bonded firmly and had a relatively uniform thickness throughout the Ti surface. This image shows how a plate-like HA layer was formed over a Ti substrate. EDS measurement of the HA coating show the Ca/P ratio is in agreement with the theoretical value Ca/P of 1.67 in HA: Ca₁₀(PO₄)₆(OH)₂. Such a bioactive layer on an implant is expected not only to enhance bony ingrowth, but also to provide a chemical integration with bone via apatite formation on its surface [17].

Figure 2 shows the XRD patterns of the ZrO₂ layer and the HA/ZrO₂ layers deposited on a Ti substrate after heat treatment at 350°C for 1 h. All diffraction peaks are assigned to the crystalline JCPDS card. XRD patterns indicated that Ti and HA peaks were predominant. The pattern clearly illustrates the HA (002) peak at $2\theta = 25.91^\circ$ and the flattened HA (211) peak at $2\theta = 31.76^\circ$. Furthermore, the flattened peak of HA indicates a coating composed of small crystallites or poor crystallinity, which is similar to natural bone minerals, and is therefore suitable for tissue compatibility [16].

3.2 Bonding strength

An HA coating, which was electrolytically deposited directly on the Ti substrate without the ZrO₂ layer, was prepared for the purpose of comparison. The bonding strength of the HA/ZrO₂ double layer coated specimen

Fig. 1 SEM micrographs of the different coating on Ti substrate after annealing at 350°C for 1 h: (a) HA/ZrO₂ coating and (b) cross-section of HA/ZrO₂ coating

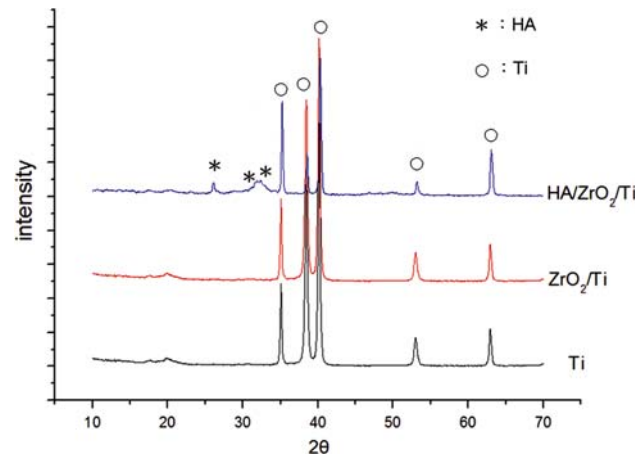
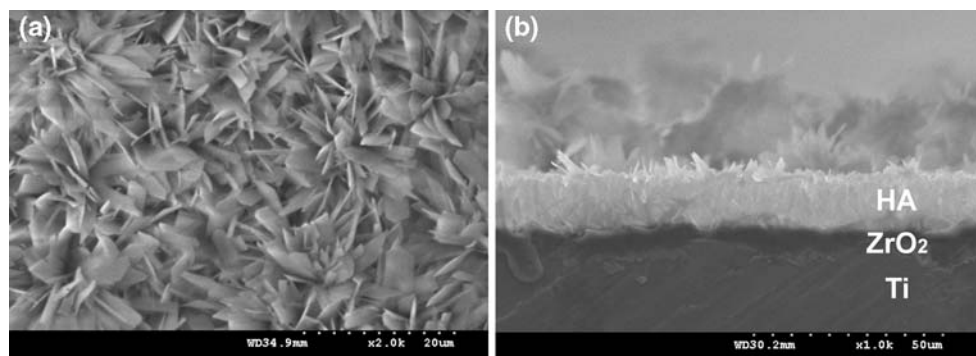


Fig. 2 XRD patterns of the ZrO₂ layer and the HA/ZrO₂ layer on Ti substrate after annealing at 350°C for 1 h

showed statistically significant differences ($P < 0.05$) from HA single layer coated specimen varying from 39.8 ± 6.2 to 28.1 ± 4.3 MPa. There was also a significant difference in the tensile strengths of the two types of specimens. The strength of the HA/ZrO₂ double layer coating was much higher than that of the HA single coating. This shows that the ZrO₂ coatings can improve the bonding strength between HA and Ti substrate. This effect is probably due to the ZrO₂ coating providing a rougher surface, which promotes a better mechanical bond between the HA coating and the ZrO₂ coating [18].

In other studies, the bonding property of plasma-sprayed HA coating on Ti alloy was reported to improve slightly with the TiO₂ layer [19]. Based on these results, it could be explained that the bonding strength of the coating layer was dependent on the substrate type. In this study, the HA layer was found to bond more strongly to the ZrO₂ layer than to the Ti substrate.

3.3 Corrosion resistance

The OCP results of Ti, ZrO₂ coated and HA/ZrO₂ coated specimens tested in artificial saliva are shown in Fig. 3. As shown in Fig. 3, the OCP curves rose rapidly before

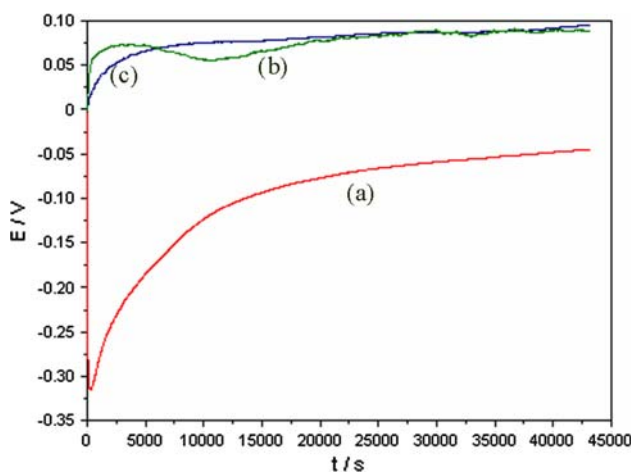


Fig. 3 OCP curves of the different coatings on Ti substrate after annealing at 350°C for 1 h: (a) Ti, (b) ZrO₂ coating, (c) HA/ZrO₂ coating

gradually reaching a stable value. All OCP curves significantly increased to positive values. The results revealed that ZrO₂ and HA/ZrO₂ coated layers would greatly affect the OCP.

The change in the corrosion potential over time is shown in Fig. 3. The stable potential of the ZrO₂/Ti and the HA/ZrO₂/Ti was approximately 0.08 V, and the stable potential of the Ti substrate was approximately -0.05 V. Although all the specimens reached a stable potential, the ZrO₂ and HA/ZrO₂ coated specimens achieved stability more rapidly than uncoated Ti substrate. This result confirms that ZrO₂, HA/ZrO₂ coating on Ti initially formed an adequate protective film. In addition, the ZrO₂ and HA/ZrO₂ coating could raise OCP to a positive value.

Slight differences in potentiodynamic polarization behavior were observed between the various surfaces for all substrates, as shown in Fig. 4. An extended passive region was observed on Ti, ZrO₂ and HA/ZrO₂ coated specimens. At the same time, ZrO₂ and HA/ZrO₂ coated on Ti substrates showed lower passive current density and higher corrosion potential than uncoated Ti substrates. This result shows that ZrO₂ and HA/ZrO₂ coated on Ti could significantly improve corrosion resistance compared to uncoated Ti.

The potentiodynamic polarization measurements made to evaluate the effect of ZrO₂ and HA/ZrO₂ coated Ti substrate are shown in Fig. 4. It can be seen that the polarization curve for ZrO₂ and HA/ZrO₂ coated Ti specimens had significantly higher ($P < 0.05$) E_{corr} values (-346 ± 56 and -379 ± 53 mV vs. SCE, respectively) than that of the uncoated sample (-518 ± 76 mV). These results confirmed that coated specimens exhibited a better electrochemical behavior than uncoated specimens because of more inert corrosion potential. There was no significant

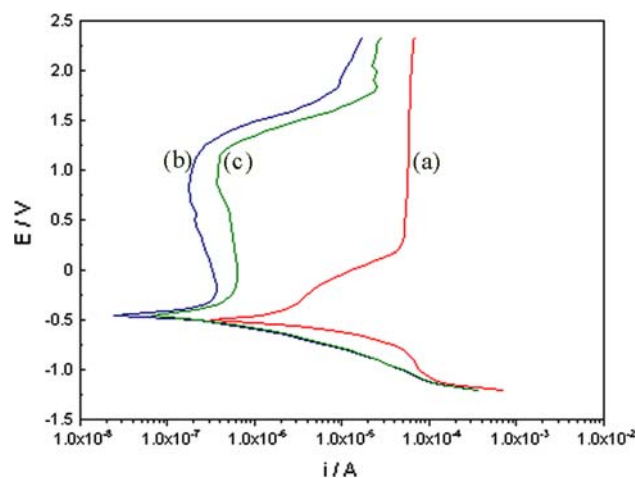


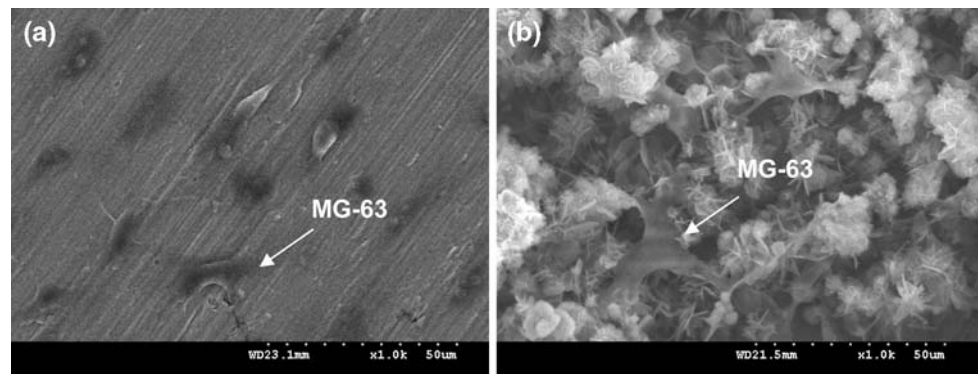
Fig. 4 Dynamic polarization curves of the different coatings on Ti substrate after annealing at 350°C for 1 h: (a) Ti, (b) ZrO₂ coating, (c) HA/ZrO₂ coating

difference in the E_{corr} values between the ZrO₂ and the HA/ZrO₂. The ZrO₂-coated, HA/ZrO₂-coated and uncoated Ti specimens had a I_{corr} of 13.9 ± 2.2 , 15.7 ± 7.6 and 184.5 ± 21.6 nA/cm², respectively. The I_{corr} values in the ZrO₂ and HA/ZrO₂ largely decreased in comparison with that of the Ti substrate, and the I_{corr} values of the ZrO₂-coated and HA/ZrO₂-coated specimens showed no significant difference ($P > 0.05$). The corrosion current density and polarization resistance (R_p) of the specimens were determined from the potentiodynamic polarization curves using the Tafel extrapolation method. The R_p values varied from 2.81 ± 0.41 (Ti) to 24.89 ± 4.03 (ZrO₂) and 24.14 ± 3.38 (HA/ZrO₂) MΩ cm², showing that the ZrO₂ and HA/ZrO₂ coatings had a better resistance to corrosion. The polarization resistance is a parameter correlated to the corrosion rate. The higher the polarization resistance, the lower the corrosion rate on the coating when exposed to artificial saliva. The potentiodynamic polarization test indicated that the ZrO₂ and HA/ZrO₂ coating had higher corrosion potential and lower passive current density than the uncoated Ti substrate. Therefore, this test confirms that the coated layers possess better corrosion resistance than the Ti substrate.

3.4 Cell culture

The biological properties of the double layer coating specimens were evaluated by observing the proliferation and differentiation of osteoblast-like MG-63 cells. Figure 5 shows SEM observation of the osteoblast-like cell MG-63 attached to two types of specimens (HA/ZrO₂-coated and uncoated Ti specimens). It shows a significant difference between the cells attached to HA/ZrO₂ coated Ti and uncoated Ti. More cells were seen to attach to the HA/ZrO₂

Fig. 5 SEM micrographs of cell growth on each specimen: (a) Ti, (b) HA/ZrO₂ coating



coated Ti, and fewer cells were found to attach to the uncoated Ti surface. These cells could attach and spread well on the HA/ZrO₂ coating surface, indicating the HA/ZrO₂ coatings possess excellent biocompatibility.

The result observed in HA/ZrO₂ specimens indicated the improvement of cell activity at an early stage. This result was probably related to the physicochemical characteristics of the different coated layers. Furthermore, the topography and surface roughness of calcium phosphate were also found to affect the adhesion, spreading, proliferation and differentiation of osteoblast-like cells. That is, the rough surface of HA/ZrO₂ coating can provide a better cell adhesion than the smooth surface of the Ti substrate might do.

4 Conclusions

This study showed that when coatings are formed on Ti substrates by the electrolytic deposition method, a ZrO₂ base layer could act as a coupling layer, by improving the bonding properties of the HA coating to the Ti substrate. It further showed that using a combination of HA and ZrO₂ coatings optimizes the biocompatibility of the Ti substrate. The HA outer layer was shown to improve bioactivity and osteoconductivity, as would occur during the initial period following implantation, and the ZrO₂ inner layer provides good corrosion resistance for the Ti substrate, even after the HA layer is completely dissolved due to biological processes. Finally, it was found that uniform and homogeneous HA/ZrO₂ coatings could be formed on Ti substrates by the electrolytic deposition method.

Acknowledgement The authors wish to gratefully acknowledge the National Sciences Council, Republic of China for supporting this research, project No. 95-2221-E-166-007.

References

1. Y.-L. Hao, M. Niinomi, D. Kuroda, K. Fukunaga, Y.-L. Zhou, R. Yang et al., *Met. Mater. Trans. A* **34A**, 100 (2003)
2. C.J. Boehlert, C.J. Cowen, C.R. Jaeger, M. Niinomi, T. Akahori, *Mater. Sci. Eng. C* **25**, 263 (2005). doi:10.1016/j.msec.2004.12.011
3. B.D. Ratner, *J. Biomed. Mater. Res.* **27**, 837 (1993). doi:10.1002/jbm.820270702
4. M.S. Block, I.M. Finger, M.G. Fontenot, J.N. Kent, *Int. J. Oral Maxillofac. Implants* **4**, 219 (1989)
5. A. Nanci, J.D. Wuest, L. Peru, P. Brunet, V. Sharma, S. Zalzal et al., *J. Biomed. Mater. Res.* **40**, 324 (1998). doi:10.1002/(SICI)1097-4636(199805)40:2<324::AID-JBM18>3.0.CO;2-L
6. J.E. Lemons, *Clin. Orthop.* **235**, 220 (1988)
7. L.L. Hench, *J. Am. Ceram. Soc.* **74**, 1487 (1991). doi:10.1111/j.1151-2916.1991.tb07132.x
8. E.J. McPherson, L.D. Dorr, T.A. Gruen, M.T. Saberi, *Clin. Orthop.* **315**, 223 (1995)
9. B.-C. Wang, E. Chang, T.-M. Lee, C.-Y. Yang, *J. Biomed. Mater. Res.* **29**, 1483 (1995). doi:10.1002/jbm.820291204
10. J. Wang, P. Layrolle, M. Stigter, K. de Groot, *Biomaterials* **25**, 583 (2004). doi:10.1016/S0142-9612(03)00559-3
11. L. Sun, C.C. Berndt, K.A. Gross, A. Kucuk, *J. Biomed. Mater. Res.* **58**, 570 (2001). doi:10.1002/jbm.1056
12. C.M. Lopatin, V. Pizziconi, T.L. Alford, T. Laursen, *Thin Solid Films* **326**, 227 (1998). doi:10.1016/S0040-6090(98)00531-8
13. W. Wenjiang, *J. Mater. Sci. Mater. Med.* **9**, 159 (1998). doi:10.1023/A:1008819703551
14. M. Gottlander, C.B. Johansson, A. Wennerberg, T. Albrektsson, S. Radin, P. Ducheyne, *Biomaterials* **18**, 551 (1997). doi:10.1016/S0142-9612(96)00168-8
15. S. Ban, S. Maruno, *Biomaterials* **16**, 977 (1995). doi:10.1016/0142-9612(95)94904-Y
16. H.-C. Hsu, S.-K. Yen, *Dent. Mater.* **14**, 339 (1998). doi:10.1016/S0109-5641(99)00002-0
17. H.-M. Kim, T. Kokubo, S. Fujibayashi, S. Nishiguchi, T. Nakamura, *J. Biomed. Mater. Res.* **52**, 553 (2000). doi:10.1002/1097-4636(20001205)52:3<553::AID-JBM14>3.0.CO;2-X
18. B.-Y. Chou, E. Chang, *Surf. Coat. Technol.* **153**, 84 (2002). doi:10.1016/S0257-8972(01)01532-8
19. H. Kurzweg, R.B. Heimann, T. Troczynski, M.L. Wayman, *Biomaterials* **19**, 1507 (1998). doi:10.1016/S0142-9612(98)00067-2